ResearchGate

See discussions, stats, and author profiles for this publication at: https://www.researchgate.net/publication/257876082

Simultaneous Open-Circuit Voltage Enhancement and Short-Circuit Current Loss in Polymer: Fullerene Solar Cells Correlated by Reduced Quantum Efficiency for Photoinduced Electron Tr...

ARTICLE *in* ADVANCED ENERGY MATERIALS · JANUARY 2013

Impact Factor: 16.15 · DOI: 10.1002/aenm.201200426

CITATIONS
33

READS
102

8 AUTHORS, INCLUDING:

Daniele Di Nuzzo
University of Cambridge
14 PUBLICATIONS **587** CITATIONS
SEE PROFILE

Ricardo K M Bouwer
Tata Steel / Delft University Of Technology
10 PUBLICATIONS **130** CITATIONS
SEE PROFILE

Stefan Meskers
Technische Universiteit Eindhoven
199 PUBLICATIONS **6,775** CITATIONS
SEE PROFILE

Paul W.M. Blom
Max Planck Institute for Polymer Research
345 PUBLICATIONS **21,975** CITATIONS
SEE PROFILE

Available from: Daniele Di Nuzzo
Retrieved on: 26 January 2016

ADVANCED ENERGY MATERIALS
www.advenergymat.de

Simultaneous Open-Circuit Voltage Enhancement and Short-Circuit Current Loss in Polymer: Fullerene Solar Cells Correlated by Reduced Quantum Efficiency for Photoinduced Electron Transfer

*Daniele Di Nuzzo, Gert-Jan A. H. Wetzelaer, Ricardo K. M. Bouwer, Veronique S. Gevaerts, Stefan C. J. Meskers, Jan C. Hummelen, Paul W. M. Blom, and René A. J. Janssen**

The limits of maximizing the open-circuit voltage V_{oc} in solar cells based on poly[2,7-(9,9-didecylfluorene)-*alt*-5,5-(4,7-di-2-thienyl-2,1,3-benzothiadiazole)] (PF10TBT) as a donor using different fullerene derivatives as acceptor are investigated. Bulk heterojunction solar cells with PF10TBT and [6,6]-phenyl-C_{61}-butyric acid methyl ester (PCBM) give a V_{oc} over 1 V and a power conversion efficiency of 4.2%. Devices in which PF10TBT is blended with fullerene bisadduct derivatives give an even higher V_{oc}, but also a strong decrease in short circuit current (J_{sc}). The higher V_{oc} is attributed to the higher LUMO of the acceptors in comparison to PCBM. By investigating the photophysics of PF10TBT:fullerene blends using near-IR photo- and electroluminescence, time-resolved photoluminescence, and photoinduced absorption we find that the charge transfer (CT) state is not formed efficiently when using fullerene bisadducts. Hence, engineering acceptor materials with a LUMO level that is as high as possible can increase V_{oc}, but will only provide a higher power conversion efficiency, when the quantum efficiency for charge transfer is preserved. To quantify this, we determine the CT energy (E_{CT}) and optical band gap (E_g), defined as the lowest first singlet state energy E_{S1} of either the donor or acceptor, for each of the blends and find a clear correlation between the free energy for photoinduced electron transfer and J_{sc}. We find that $E_g - qV_{oc} > 0.6$ eV is a simple, but general criterion for efficient charge generation in donor-acceptor blends.

1. Introduction

Polymer solar cells will contribute to future renewable energy production when high efficiencies can be combined with low-cost large-area production and long lifetimes. The most efficient polymer solar cells to date use an active layer that consists of a bulk heterojunction in which electron donor and electron acceptor materials are mixed on a nanometer scale. In recent years, a myriad of semiconducting donor polymers has been developed that have provided polymer solar cells with power-conversion efficiencies (PCEs) exceeding 8% in single and tandem junctions.[1–5] Virtually all polymer solar cells employ a fullerene derivative, [6,6]-phenyl-C_{61}-butyric acid methyl ($PC_{61}BM$) or its C_{70} analogue ($PC_{71}BM$), as the electron acceptor.

To further enhance the performance of polymer solar cells, judicious design of new materials in terms of frontier energy levels, charge-carrier mobility, and morphology is becoming increasingly important. For this purpose, design rules are required. It is by now well established that the maximum open-circuit voltage (V_{oc}) delivered by bulk heterojunction polymer:fullerene solar cells is determined by the difference between the energy of the lowest unoccupied molecular orbital (LUMO) of the electron acceptor and the energy of the highest occupied molecular orbital (HOMO) of the electron donor.[6–8] Hence, a strategy to increase power-conversion efficiency is to engineer acceptors with a LUMO energy that is as high as possible, since this would result in higher a V_{oc}. This approach has been successfully applied to solar cells

D. Di Nuzzo, V. S. Gevaerts, Dr. S. C. J. Meskers, Prof. R. A. J. Janssen
Molecular Materials and Nanosystems
Eindhoven University of Technology
PO Box 513, 5600 MB Eindhoven, The Netherlands
E-mail: r.a.j.janssen@tue.nl
G. A. H. Wetzelaer, Prof. P. W. M. Blom
Molecular Electronics and Zernike Institute for Advanced Materials
University of Groningen
Nijenborgh 4, 9747 AG Groningen, The Netherlands
Dr. R. K. M. Bouwer, Prof. J. C. Hummelen
Stratingh Institute for Chemistry and Zernike Institute for Advanced Materials
University of Groningen
Nijenborgh 4, 9747AG Groningen, Netherlands
D. Di Nuzzo, V. S. Gevaerts, G. A. H. Wetzelaer, Dr. R. K. M. Bouwer
Dutch Polymer Institute
P.O. Box 902, 5600 AX, Eindhoven, The Netherlands

DOI: 10.1002/aenm.201200426

© 2012 WILEY-VCH Verlag GmbH & Co. KGaA, Weinheim

containing poly(3-hexylthiophene) (P3HT) as electron donor by using fullerene bisadducts as acceptors.[9–12]

In a HOMO-LUMO band diagram the intuitive limit of raising the acceptor LUMO level would be the case where the difference between the LUMO levels and HOMO levels of the donor and acceptor would become less than the exciton binding energy on donor or acceptor, which for many organic materials would be typically around 0.4 eV. However, this design criterion is oversimplified: increasing the acceptor LUMO also increases the donor-acceptor HOMO-LUMO offset that in turn determines the energy (E_{CT}) of the charge-transfer (CT) state that should be formed in the photoinduced electron transfer reaction between electron donor and acceptor.[8,13] The CT state has an important role in organic solar cells because it is a precursor state in forming free charges. Energetically, the CT state must be below the singlet exciton (S_1) energies (E_{S1}) of both the donor and the acceptor to be formed in appreciable yield under illumination. By increasing the donor-acceptor HOMO-LUMO offset, the E_{CT} will eventually be above the E_{S1} states, inhibiting charge formation. E_{CT} has been identified in various donor-acceptor blends via photoluminescence (PL), electroluminescence (EL), photothermal-deflection absorption spectroscopy, and by measuring the wavelength dependence of the photocurrent.[14–16] From these studies, it has become clear that V_{oc} and E_{CT} are directly related.

To investigate the limits of increasing the V_{oc} versus efficiency of charge formation, we consider polymer solar cells based on poly[2,7-(9,9-didecylfluorene)-*alt*-5,5-(4,7-di-2-thienyl-2,1,3-benzothiadiazole)] (PF10TBT) (**Figure 1**). PF10TBT is a copolymer with a wide band gap (E_g = 1.95 eV) that, combined with PCBM, gives a PCE of 4.2% and a high V_{oc} of 1 V under 1 sun illumination.[17] Optimized PF10TBT:PCBM solar cells have an internal quantum efficiency (IQE) of 75%.[17] We investigate PF10TBT blended with PCBM and fullerene derivatives having higher LUMO energies, namely bis-PCBMs[9] and indene-C_{60}-bisadduct (ICBA)[10] (Figure 1). For bis-PCBM the LUMO is about 100 mV higher than that of PCBM and for ICBA the increase is about 190 mV.[9,11] Bis-PCBM, like all fullerene bisadducts, is commonly obtained as a mixture of regio- and stereoisomers and in this study we compare three samples of bis-PCBM that differ in the number of isomers. We blend these different fullerene derivatives with PF10TBT to gain information on the efficiency of charge transfer relative to the free energy for photoinduced charge transfer by means of steady state near-IR PL and EL, time-resolved PL, and photoinduced absorption (PIA) spectroscopy, and compare the results with the performance of the PF10TBT:fullerene solar cells. The similarity in chemical structure between the various acceptors allows us to establish a clear correlation between photogenerated current and energy of the S_1 and CT states. When using the optical band gap (E_g), defined as the lowest first singlet state energy E_{S1} of either the donor or acceptor, as a measure for the lowest optically accessible state, we find that for an $E_g - E_{CT}$ energy difference of less than +100 meV, CT-state formation and generation of free charge carriers are significantly reduced.

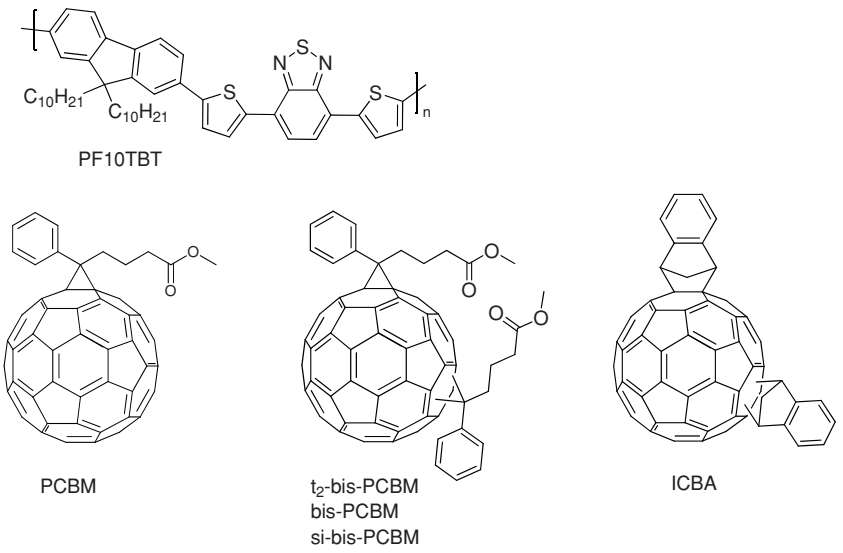

Figure 1. Structure of PF10TBT and the fullerene derivatives used. For bis-PCBM three different regio- and stereoisomer mixtures (t_2-bis-PCBM, bis-PCBM, and si-PCBM) where used (see text).

2. Results and Discussion

2.1. Materials

In this study we compare PCBM, bis-PCBM, and ICBA (Figure 1). HPLC analysis shows that synthesized bis-PCBM consists of at least 15 different isomers out of the 22 possible regio- and stereoisomers.[18,19] A smaller selection of isomers is the mixture t_2-bis-PCBM that was synthesized using a ethylene tether between the 4-phenylbutyric acid moieties to control their mutual position on the fullerene. After transesterification with methanol, t_2-bis-PCBM was found to contain 7 different isomers.[18] Finally, a small sample of a single isomer, si-bis-PCBM, was obtained by separation from the standard bis-PCBM isomer mixture using preparative HPLC.[20] Compared to PCBM the reduction potentials of the bis-PCBMs and ICBA are more negative and, hence, their higher LUMO levels are expected to increase the V_{oc} of the solar cell. The reduction potentials vs. Fc/Fc^+ are collected in **Table 1**.

Table 1. Characteristics of PF10TBT:fullerene solar cells.

Fullerene	V_{oc} (V)	J_{sc} (A/m^2)	FF	PCE (%)	E_{red}[a)]
PCBM	1.005	68.6	0.60	4.14	–1.09
t_2-bis-PCBM	1.114	29.6	0.46	1.51	–1.18
bis-PCBM	1.127	25.3	0.45	1.27	–1.19
si-bis-PCBM	1.163	20.3	0.47	1.11	–1.15
ICBA	1.173	4.0	0.42	0.20	–1.28

[a)] Reduction potential vs. Fc/Fc^+.

© 2012 WILEY-VCH Verlag GmbH & Co. KGaA, Weinheim

DOI: 10.1002/aenm.201200426

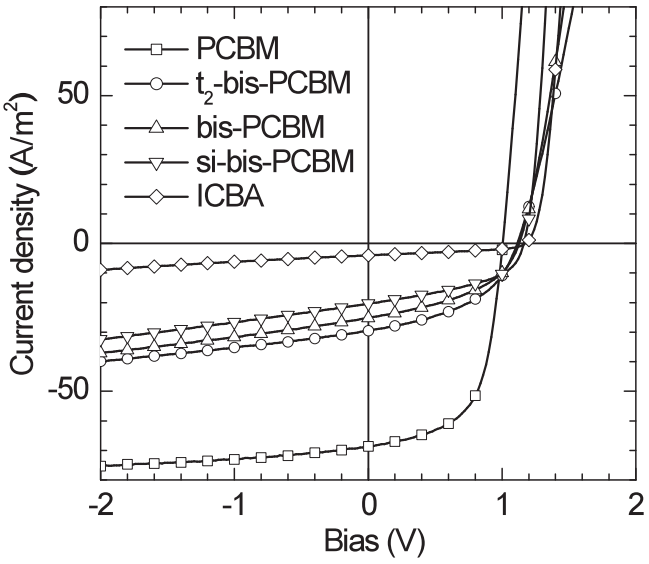

Figure 2. Current density–voltage (*J–V*) characteristics of solar cells based on PF10TBT as electron donor blended with the different fullerene acceptors (see legend). The PF10TBT:fullerene weight ratio is 1:4 for all cells.

2.2. Solar Cells

The *J–V* curves of the solar cells made from the five different PF10TBT:fullerene blends in 1:4 weight ratio with ITO/PEDOT:PSS and LiF/Al electrodes are shown in **Figure 2** and the device parameters are summarized in Table 1. For PF10TBT:PCBM, a PCE of 4.1% was obtained, which is close to optimal for this system.[17] The V_{oc} of 1.005 V for the PF10TBT:PCBM cell is high. Interestingly, Figure 2 shows that V_{oc} can be further increased by using bis-PCBM or ICBA. The highest V_{oc} of 1.173 V was obtained for PF10TBT:ICBA, *i.e.* for the bulk heterojunction incorporating the acceptor with the highest LUMO level. As can be seen in Figure 2, the increase in V_{oc} for the PF10TBT cells based on the fullerene bisadducts is accompanied by a dramatic decrease of the short-circuit current density (J_{sc}) and, hence, a strong decrease in PCE. We note that for all samples the increase in current density under illumination going from 0 to –2 V is very similar. This indicates that the loss in current is not primarily due to stronger field dependence in charge generation or transport in this bias regime. Further the intrinsic electron mobilities of bis-PCBM and ICBA are not limiting the performance of their cells with PF10TBT either, as very efficient operation of these derivatives was reported with P3HT.[9,11]

To investigate if morphology differences of the PF10TBT:fullerene blends can rationalize the observed differences in current density, we studied the phase separation in the photoactive blends with bright-field transmission electron microscopy (TEM). **Figure 3** illustrates that the morphology of all layers is very similar. The darker areas in the TEM correspond to fullerene rich areas and suggest that fullerene domains of 50-100 nm are present for PF10TBT:PCBM and the PF10TBT:bis-PCBMs. The morphologies of the blends of PF10TBT with PCBM and three bis-PCBM blends are virtually indistinguishable (Figure 3). From this we conclude that differences in morphology are unlikely the main cause of the differences in performance of the solar cells. Only for PF10TBT:ICBA the fullerene domains appear to be larger (100–150 nm). Although we have no detailed information on the composition of the darker domains, we consider it unlikely that these are pure in fullerene.

Because the differences in morphology are relative small, we consider that factors such as exciton migration to the donor-acceptor interface and percolation of photogenerated charges

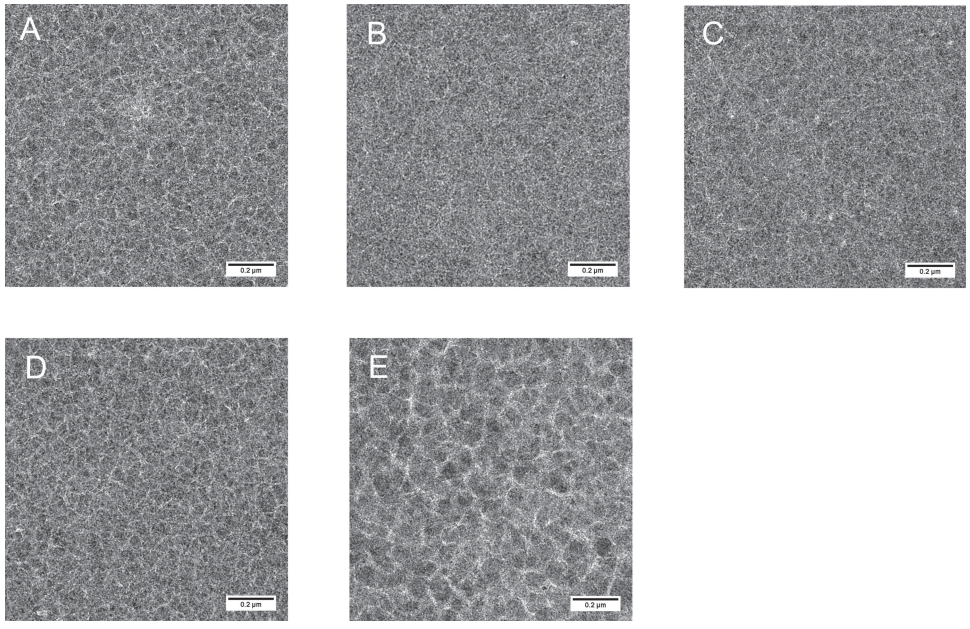

Figure 3. Bright field TEM images of layers containing PF10TBT mixed with (a) PCBM, (b) t_2-bis-PCBM, (c) bis-PCBM, (d) si-bis-PCBM, and (e) ICBA. The bar represents 0.2 µm.

© 2012 WILEY-VCH Verlag GmbH & Co. KGaA, Weinheim

to the electrodes are unlikely to be strongly different for the blends.

2.3. Steady State Near-IR Luminescence

A possible reason for the decrease in photocurrent for PF10TBT:bis-PCBM and PF10TBT:ICBA is a reduction of the quantum yield of formation of the CT state under illumination. For PF10TBT:PCBM, a clear signature of formation of the CT state is the detectable CT luminescence in which the CT state recombines radiatively to the ground state.[14,21] We use this property to investigate the charge-transfer step in all the blends under study.

Figure 4a shows the normalized PL spectra of a pristine PF10TBT film (green line), of PCBM in toluene solution (blue line), and of a PF10TBT:PCBM blend (black line). The films were excited using 2.21 eV photons, exciting both the polymer and the fullerene. The PL of pristine PF10TBT is characterized by a spectrum peaked at 1.79 eV. PCBM has a PL spectrum with two vibronically coupled peaks at 1.75 and 1.58 eV. When PF10TBT and PCBM are blended, the polymer luminescence is quenched by a factor of ~10^3. The remaining PL is completely different from the emission of the single compounds and is characterized by a broad spectrum, peaked at 1.52 eV, that can be attributed to CT emission. The PL spectrum of the blend shows a small residual, blue-shifted, fluorescence of PF10TBT at ~1.9 eV.

Figure 4b shows the results of the same experiments using PF10TBT:t_2-bis-PCBM. The PL of the blend film has two peaks respectively at 1.65 and 1.50 eV, with a spectral shape and position that is very similar to the emission of the acceptor t_2-bis-PCBM in toluene. For blends of PF10TBT with bis-PCBM, si-bis-PCBM, or ICBA, photoluminescence spectra with a band shape very similar to PF10TBT:t2-bis-PCBM are obtained (Figures 4c–e). For none of the PF10TBT:fullerene bisadduct films CT luminescence is clearly distinguishable. For the PF10TBT blends with fullerene bisadducts, we attribute the PL to fluorescence from the S_1 excited state of the fullerene acceptor. In the series t_2-bis-PCBM, bis-PCBM, si-bis-PCBM, and ICBA the relative amount of residual polymer fluorescence increases, with the intensity rising from ~10^{-3} to ~10^{-2} relative to fluorescence of pristine PF10TBT.

These observations suggest that only the blend containing PCBM has an efficient photoinduced charge transfer between PF10TBT and the polymer, whereas with the other acceptors the charge-transfer efficiency is significantly reduced. By raising the LUMO of the fullerene, the CT state energy increases and approaches the fullerene S_1 energy, reducing the overall exciton dissociation efficiency and creating exergonic pathways for charge recombination of holes in PF10TBT and electrons in the fullerene, to form the fullerene S_1 state. Similar results were recently shown in literature.[22] Of course we cannot rule out that the CT is formed initially, but that (back) electron transfer from CT state to pure fullerene bisadduct excited state is fast as compared to dissociation of the CT state into free charge carriers.

To study the energy difference between CT and fullerene S_1 states in more detail, we recorded electroluminescence of the PF10TBT:fullerene blends sandwiched between ITO/PEDOT:PSS and LiF/Al electrodes. Because of lack of sufficient material it was not possible to fabricate PF10TBT:si-bis-PCBM additional devices for this experiment. **Figure 5** shows the *J*–*V* and light output–*V* characteristics for four PF10TBT:fullerene

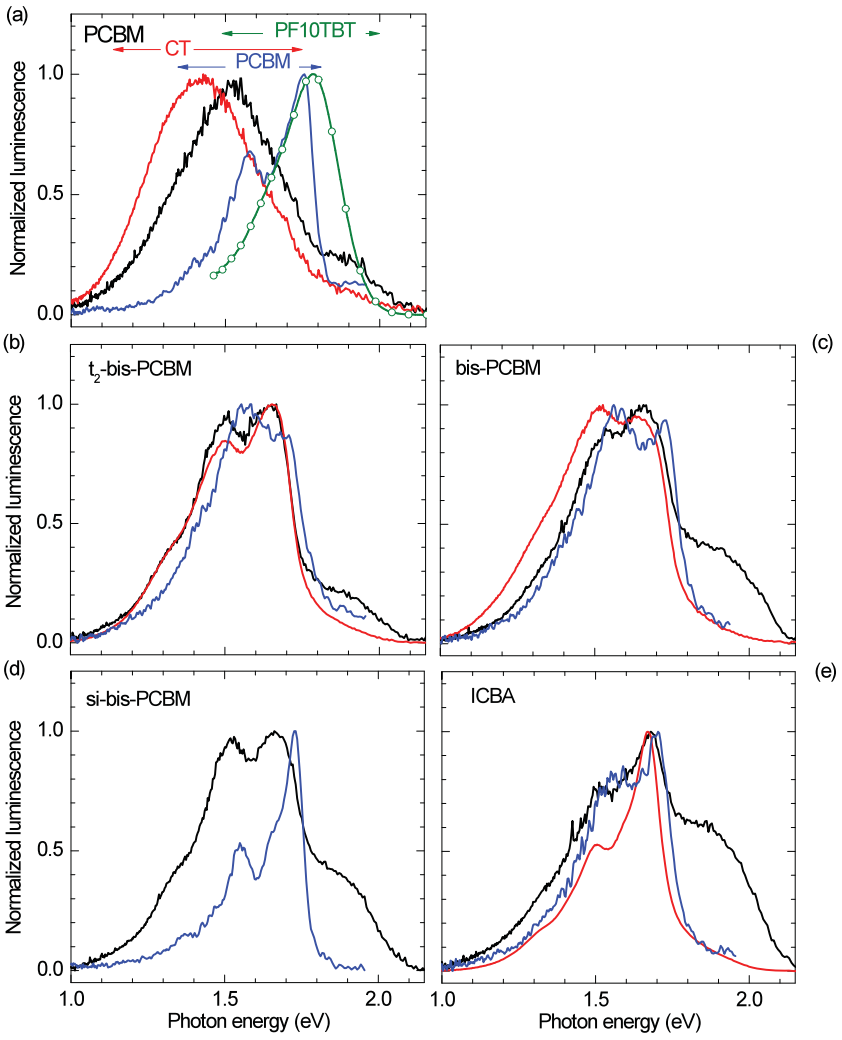

Figure 4. Comparison between the photoluminescence (PL) spectra of thin films (black lines) and electroluminescence (EL) spectra (3 V forward bias) of solar cells (red lines) of blends of PF10TBT with different fullerene acceptors (see legends). In each panel the PL of the fullerene acceptor in toluene solution is shown (blue lines). Thin films were excited at E_{exc} = 2.21 eV, solutions at E_{exc} = 2.38 eV. For si-bis-PCBM the EL spectrum could not be recorded because of lack of sufficient material. Panel (a) also shows the photoluminescence spectrum of a pristine PF10TBT film (green line).

© 2012 WILEY-VCH Verlag GmbH & Co. KGaA, Weinheim

DOI: 10.1002/aenm.201200426

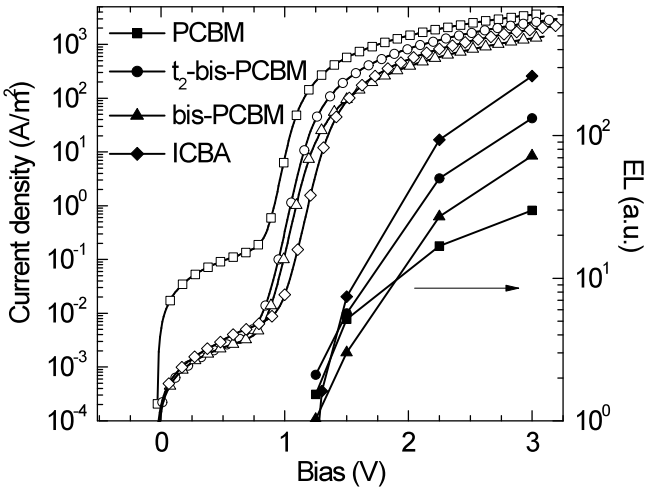

Figure 5. Semi-logarithmic plot of the *J–V* characteristics of PF10TBT:fullerene devices (open symbols) and the electroluminescence (EL) intensities (closed symbols) under forward bias obtained by integrating over the emission spectrum.

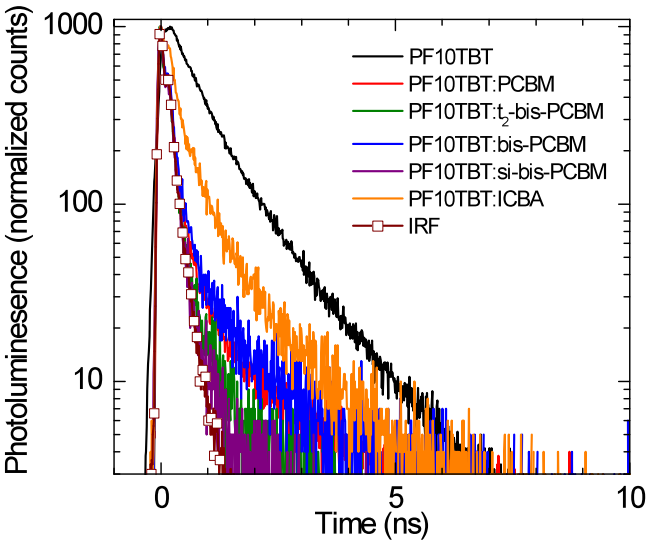

Figure 6. Time-resolved photoluminescence of PF10TBT in pristine film and in PF10TBT:fullerene films recorded for E_{em} = 1.97 eV with E_{exc} = 3.06 eV at room temperature. The instrument response function (IRF) is shown. The emission of pristine PF10TBT can be fitted with a three-exponential curve with lifetimes τ = 0.3, 0.8, and 1.6 ns, accounting for 25%, 50%, and 25% of the emission, respectively.

blends. The onset of light emission at ~1.2 V roughly matches with a sharp rise in dark current density (0.9–1.1 V). For pure PF10TBT layers, the onset of current and light output occurs at higher potentials (~1.8 V).[21] The voltage at which the dark current density increases, scales with the V_{oc} of the cells and hence corresponds to injection of holes in the HOMO of PF10TBT and of electrons in the LUMO of the fullerene. Recombination of holes and electrons at the PF10TBT-fullerene interface is therefore expected to form primarily, and certainly initially, the CT state.

Figures 4a–e show the normalized electroluminescence (EL) spectra recorded at forward bias (+3V) (red lines). In each case, the EL spectrum closely matches the PL spectrum. With PCBM, luminescence from the PF10TBT:PCBM CT state is indeed observed (red shifted compared to the PL). This suggests that the CT state has the lowest energy among all excited states in that blend. For all bisadducts, however, the EL spectrum of the blends is dominated by fullerene bisadduct emission. Apparently, electron-hole recombination does not give rise to CT emission, but rather emission from the fullerene singlet S_1 state, which has been rapidly formed from the initial CT state. The small differences observed between the EL and the PL spectra in Figure 4 can be due to the different way the states are populated compared to the PL and to different out-coupling of light.

2.4. Time-Resolved Photoluminescence

To further investigate the differences in the photophysics of the blends, we performed time-resolved PL experiments that may reveal individual contributions from PF10TBT and PCBM S_1 states and their CT state via different lifetimes. **Figure 6** shows the decay traces of the PL from a PF10TBT pristine film and from PF10TBT:fullerene blends, using 3.06 eV as excitation photon energy. The instrument response function (IRF) is also plotted. The emission was recorded at 1.97 eV, where the steady state spectra show some polymer residual fluorescence in the blends (Figure 4). The PL decay of the pristine PF10TBT film is characterized by a distribution of lifetimes.

In the PF10TBT:fullerene blends the fluorescence from the polymer is significantly quenched. The fluorescence decay generally occurs on a very fast time scale, close to the IRF, which precludes a quantitative analysis. Only for the PF10TBT:ICBA blend we find a decay that is slower than the IRF and contains a long-lived component that resembles the decay observed in the PF10TBT pristine film. This indicates that in PF10TBT:ICBA blends, some excitations on the polymer are not quenched. Likely, this is a consequence of a somewhat stronger phase separation (Figure 3).

Figure 7 depicts the PL decay traces of the PF10TBT:fullerene blends with excitation at 3.06 eV and detection at 1.65 eV and compares these with the decay traces of pristine fullerene films at the same photon energies. At 1.65 eV emission from both the fullerene S_1 state and the CT state can be expected. The traces were fitted to multi-exponential functions and the parameters extracted from the fits are summarized in **Table 2**. The pristine fullerenes show single exponential fluorescence decays in thin films with lifetimes between 0.77 and 1.52 ns.

Blending PCBM with PF10TBT changes the dynamics of the fluorescence completely (Figure 7a). The blend shows a three-component decay: a fast component (80 ps, in the order of the instrument time resolution), a second one of 0.5 ns and a relatively long lived third one (3 ns). The first component is assignable to residual polymer fluorescence, consistent with the emission observed at 1.97 eV (Figure 6). The two latter components are assignable to the S_1 decay of PCBM and the CT-state decay.[14,21]

© 2012 WILEY-VCH Verlag GmbH & Co. KGaA, Weinheim

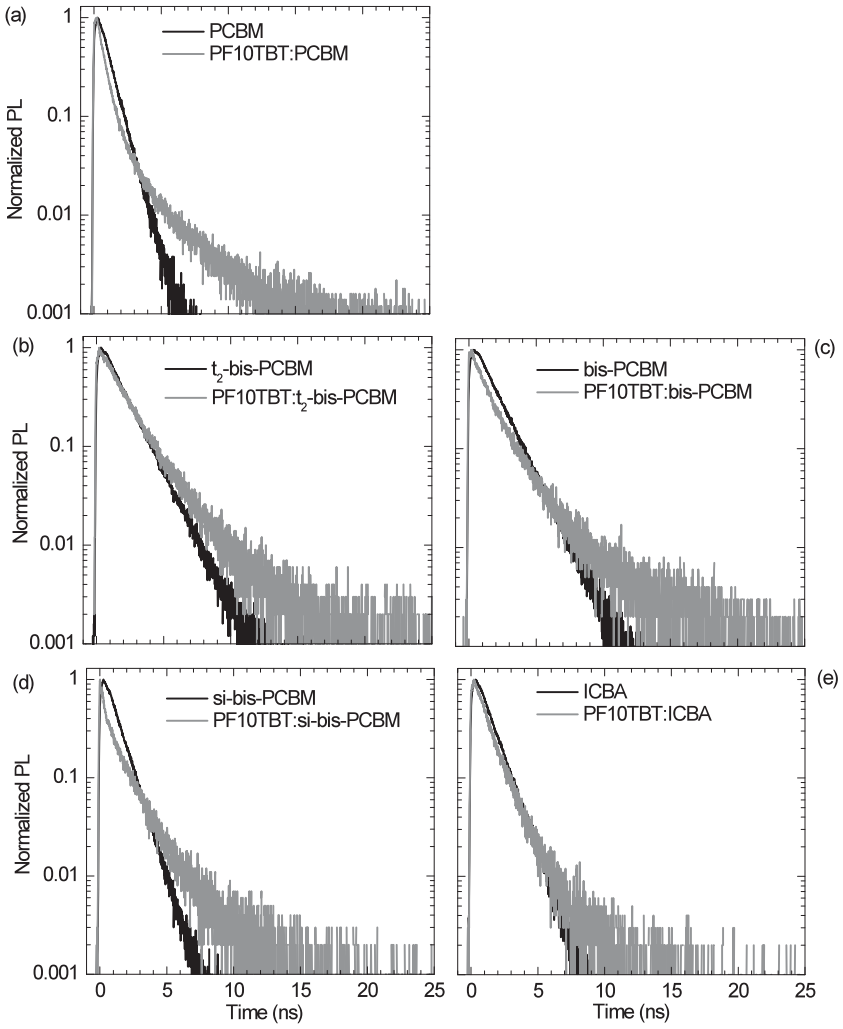

Figure 7. Time-resolved photoluminescence of fullerenes in pristine films (black lines) (a) PCBM, (b) t_2-bis-PCBM, (c) bis-PCBM, (d) si-bis-PCBM, and (e) ICBA compared to the photoluminescence of the same fullerene acceptors when blended with PF10TBT (gray lines). Spectra were recorded for E_{em} = 1.65 eV with E_{exc} = 3.06 eV at room temperature.

Table 2. Fit parameters of the time-resolved PL decay traces.[a)]

	τ_1 (ns)	α_1 [b)]	τ_2 (ns)	α_2 [b)]	τ_3 (ns)	α_3 [b)]	χ^2
PCBM	0.77	1					0.690
PF10TBT: PCBM	0.08	0.198	0.58	0.614	3.02	0.188	1.186
t_2-bis-PCBM	1.52	1					0.733
PF10TBT: t_2-bis-PCBM	0.03	0.048	1.57	0.757	3.28	0.195	0.570
Bis-PCBM	1.50	1					0.726
PF10TBT: Bis-PCBM	0.03	0.102	1.26	0.672	3.32	0.226	0.620
si-bis-PCBM	0.96	1					0.648
PF10TBT: si-bis-PCBM	0.03	0.238	1.22	0.593	3.11	0.169	0.450
ICBA	1.09	1					0.617
PF10TBT: ICBA	0.05	0.072	0.88	0.650	1.78	0.278	0.447

[a)]Recorded at E_{em} = 1.65 eV with E_{exc} = 3.06 eV; [b)]α_i is the lifetime weighted fractional intensity of each component of the multi-exponential fit.

The t_2-bis-PCBM and bis-PCBM acceptors show a different behavior, with fluorescence decays that do not change as strongly as for PCBM when going from the pristine film to the blend. This is not unexpected because the steady state PL spectra are dominated by fullerene fluorescence. Again, three components appear: a first one below the instrument response time (<80 ps), a second one between 1 and 1.5 ns, and a longer lived one above 3 ns. As with PCBM, the first short component is coming from some residual polymer fluorescence, but in these cases its lifetime weighted fractional intensity (α < ~0.1) is lower than for PCBM (α ~ 0.2). An exception is the blend containing si-bis-PCBM, where the first fast component has α ~ 0.25, comparable with to the PF10TBT:PCBM blend. The second component, however, is similar in all the cases to the pristine films lifetimes (1–1.5 ns) and we assign it to the decay of the fluorescence from the acceptors. The third longer component is in the same range (3 ns) as the one observed in PF10TBT:PCBM and we interpret it to originate from CT emission.

The time-resolved PL of the pristine ICBA acceptor and the PF10TBT:ICBA film show the strongest resemblance. Also in this case the curve was best fitted with a three-exponential decay, which resulted in a fast component (50 ps) having a very small α and two longer components, respectively 0.88 and 1.78 ns, that we can attribute to the decay of fluorescence from the acceptor itself (1.09 ns mono-exponential in the pristine film). The 3 ns long-lived decay time associated with CT emission and observed in all other blends is not present in this case.

The time-resolved PL results show that some long-lived CT emission occurs in the blends of PF10TBT with the three bis-PCBM isomer mixtures, but less compared to PCBM. Likely, also in the steady state PL spectra, emission from the CT state is present, but buried under the emission of the acceptors. For PF10TBT:ICBA, instead, there is no evidence for charge transfer from either steady state or time-resolved PL.

2.5. Photoinduced Absorption

Photoinduced absorption (PIA) spectroscopy can be used to probe the formation of free charges or excited states and provide additional information on the photophysical processes occurring in the blends. We recorded PIA spectra for films of pristine PF10TBT

© 2012 WILEY-VCH Verlag GmbH & Co. KGaA, Weinheim
Adv. Energy Mater. 2012,
DOI: 10.1002/aenm.201200426

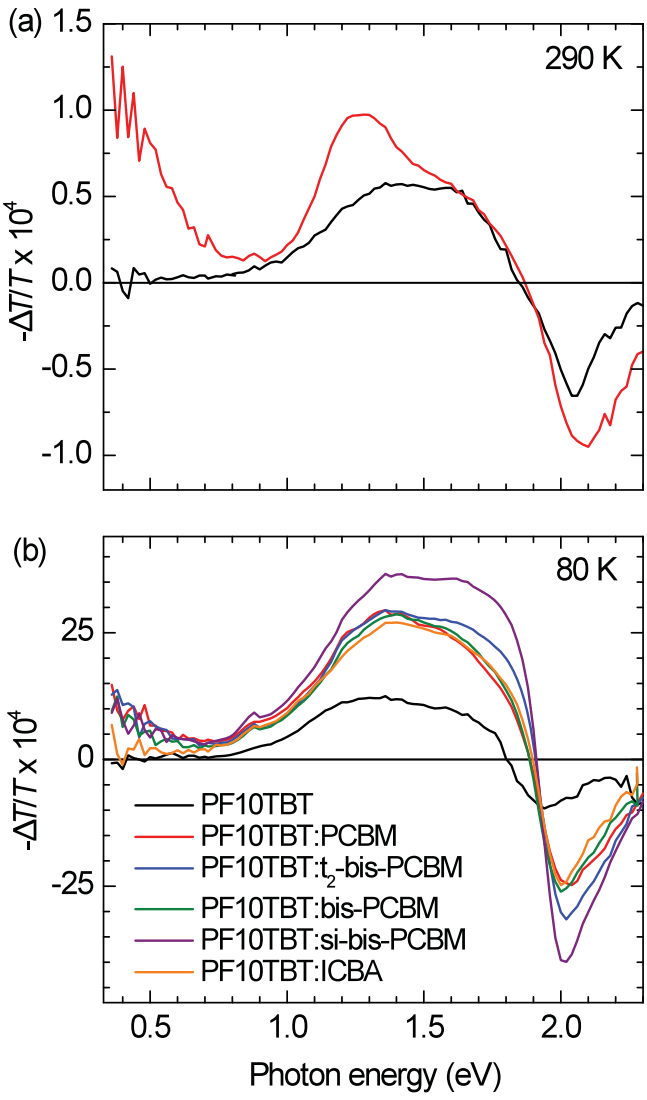

Figure 8. Near steady state PIA spectra of pristine PF10TBT and mixed PF10TBT:fullerene films (see legend). (a) Recorded at 290 K. (b) Recorded and 80 K. Excitation at $E_{exc} = 2.41$ eV.

and mixed PF10TBT:fullerene blends at room temperature and 80 K (**Figure 8**). The PIA spectrum of the pristine PF10TBT film at room temperature shows a broad band between 1.0 and 1.8 eV with a broad maximum centered at 1.5 eV (Figure 8a). This band is attributed to the $T_n \leftarrow T_1$ transition of PF10TBT, where T_1 is the lowest triplet state in the polymer.[21,23] When PF10TBT is blended with PCBM, the PIA spectrum exhibits two new bands at 1.25 and at ~0.5 eV. These two bands are comparable in intensity and are a signature of long lived charges on PF10TBT.[21,24]

At 80 K, the spectrum of pure PF10TBT (Figure 8b) has increased in intensity because the lifetime of the T_1 state has increased. For the PF10TBT:PCBM blend, the PIA spectrum is now dominated by a strong $T_n \leftarrow T_1$ transition, although the signal at ~0.5 eV of charges remains clearly visible. In the near-steady state PIA technique, the signal intensity is proportional to the lifetime (as one probes a steady state concentration) and the increase of the $T_n \leftarrow T_1$ transition for pristine PF10TBT is due to a longer lifetime.[21] The fact that the T_1 signal intensity in the PF10TBT:PCBM blend is about twice that of the pristine film, indicates that recombination of (some) CT states into the PF10TBT T_1 state occurs at the interface. The recombination to the triplet state is consistent with triplet state energy of PF10TBT of ~1.4 eV[21] being less than that of the CT state (1.48 eV, **Table 3**). Charge recombination to the triplet state represents an additional loss mechanism, and has been indentified in various material combinations.[25–29]

Table 3. Open circuit voltage and CT state energies of PF10TBT:fullerene blends.

Fullerene	V_{oc} (V)	E_{CT} (eV)[a)]	E_g (eV)[b)]	E_g–E_{CT} (eV)
PCBM	1.005	1.48	1.66	0.18
t_2-bis-PCBM	1.114	1.58	1.66	0.08
bis-PCBM	1.127	1.60	1.65	0.05
si-bis-PCBM	1.163	1.63	1.66	0.03
ICBA	1.173	1.64	1.63	–0.01

[a)]From Equation (1); [b)]E_g in the blend.

For the three bis-PCBM samples, the PIA spectra of blends with PF10TBT are virtually identical to that of PF10TBT:PCBM. The triplet signal is between 20 and 30 times higher than at room temperature and in all cases it is stronger than in the pristine PF10TBT film. This shows that also with bis-PCBMs recombination of the CT state to the PF10TBT T_1 state competes with dissociation in long-lived charge carriers. In contrast, the PF10TBT:ICBA blend shows almost no signatures from charges at ~0.5 eV, consistent with very limited photocurrent extracted from the devices and in agreement with the luminescence experiments.

The triplets observed in the PIA spectrum of PF10TBT:ICBA likely originate via triplet energy transfer from the triplet state of ICBA, formed via intersystem crossing from the singlet state. The same process likely also occurs in the blends containing the different bis-PCBM isomeric mixtures, where the singlet state of the acceptor is not completely depopulated by charge transfer.

2.6. Energy of the CT and S_1 states in PF10TBT: Fullerene Blends

To explain the increase in V_{oc} and the concomitant loss in J_{sc}, and to rationalize the outcome of the photophysical experiments, it is useful to consider the energetics of the PF10TBT:fullerene blends in more detail. We will follow the approach of Veldman *et al.*, who developed an empirical relation to estimate the CT energy at room temperature:[13]

$$E_{CT} = q\,V_{oc} + 0.47\text{eV} \quad (1)$$

in which V_{oc} is the value at room temperature and 1 sun illumination and q the elementary charge. Relations similar to Equation (1) have been described by Vandewal et al.[8,15]

Table 3 summarizes the E_g and CT (E_{CT}) energies of the blends containing PF10TBT and the different fullerene

© 2012 WILEY-VCH Verlag GmbH & Co. KGaA, Weinheim

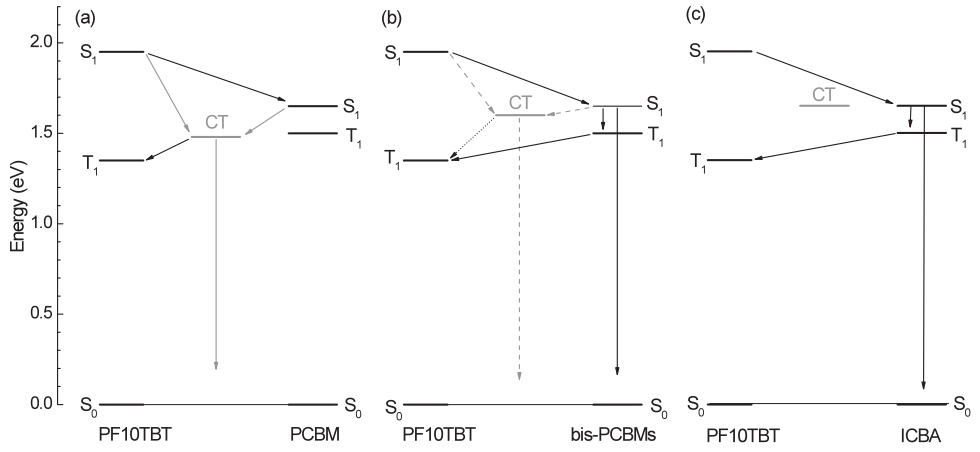

Figure 9. Jablonski diagram of the transitions that occur after photoexcitation in the PF10TBT:fullerene blends for (a) PCBM, (b) bis-PCBM isomeric mixtures, and (c) ICBA. Note that the CT energy rises from (a) to (c). Solid lines represent dominant processes, dashed lines represent minor processes.

acceptors, estimated using Equation (1). We note that in each case E_g equals E_{S1} of the acceptor. Table 3 reveals that while the S_1 energy of the different fullerene derivatives is almost invariant around 1.65 eV and significantly less than that of PF10TBT at 1.95 eV, the CT energy increases from PCBM, via the bis-PCBMs, to ICBA. The rise in CT energy is a consequence of the more negative reduction potential and, hence, higher LUMO energy of the higher adducts. As a consequence of these effects, the free energy for photoinduced electron transfer, defined as $\Delta G_{CT} = E_{CT} - E_g$, decreases from about –0.2 eV for PF10TBT:PCBM, via –0.1 eV for the three bis-PCBM blends with PF10TBT, to almost 0 eV for PFT10TBT:ICBA (Table 3). The increase of ΔG_{CT} eventually inhibits the photoinduced electron transfer between PF10TBT and the fullerene bisadducts and explains the loss in J_{sc}. It is remarkable to see that the trend in ΔG_{CT} accurately follows the trend in J_{sc} for all five acceptors. The Jablonski diagrams in **Figure 9** summarize the transitions taking place in the blends containing the different acceptors after photoexcitation.

Interestingly, the present results are in accurate agreement with the empirical predictions previously made by Veldman *et al.* based on the study of a broad range of donor-acceptor blends, where photoinduced charge transfer was found to be efficient when $\Delta G_{CT} = E_{CT} - E_g < -0.1$ eV.[13] Vandewal *et al.* recently described a similar result.[30] This energetic estimate also explains the observations made in photoluminescence and electroluminescence. CT emission was clearly identified for PF10TBT:PCBM, but was less evident for the three PF10TBT:bis-PCBM blends, and virtually absent for PF10TBT:ICBA. The fact that the electroluminescence spectra of the PF10TBT:fullerene bisadduct blends mainly show fullerene emission, evidences that a CT state, initially formed by capturing an electron and hole at the PF10TBT:fullerene bisadduct interface, can populate the fullerene bisadduct S_1 state, which emits radiatively or intersystem crosses to its T_1 state.

Finally, we note that the offset E_g-E_{CT} follows the same trend as the short-circuit currents observed in the devices and of the charge transfer efficiency as suggested by the time resolved PL measurements. This correlation indicates the importance of the population of bound CT states as a first step in the generation of free charges in these blends.

3. Conclusion

When PF10TBT is blended with C_{60} bisadducts (bis-PCBM in three different isomeric selections and ICBA) in bulk heterojunction solar cells the open-circuit voltage (V_{oc}) is increased compared to PCBM as electron acceptor. A simultaneous dramatic loss in short-circuit current (J_{sc}), however, results in a reduced power-conversion efficiency. By using photoluminescence and photoinduced absorption spectroscopy, we have identified that the principal reason for the loss in J_{sc} is the fact that photoinduced charge transfer becomes increasingly more impeded when going from PCBM, via the bis-PCBMs, to ICBA. Electroluminescence experiments revealed that the S_1 states of bis-PCBM and ICBA can be formed subsequent to electron-hole recombination at the PF10TBT-bisfullerene interface.

We have found a clear correlation between the efficiency of charge transfer and the free energy for photoinduced charge generation $\Delta G_{CT} = E_{CT} - E_g$, where E_g is the lowest optical band gap among donor and acceptor. In fact, in our experiments ΔG_{CT} correlates with J_{sc}. Triplet formation is an additional loss channel for all PF10TBT:fullerene blends. PF10TBT T_1 states can be formed from the CT state by charge recombination as observed in PF10TBT:PCBM or via intersystem crossing ($S_1 \rightarrow T_1$) of the fullerene S_1 state and subsequent triplet energy transfer to PF10TBT, which prevails in the PF10TBT:ICBA blend.

In this work we have obtained a clear confirmation of the measure for efficient photoinduced electron transfer in donor-acceptor bulk heterojunctions in terms of the free energy: $\Delta G_{CT} = E_{CT} - E_g < -0.1$ eV. Because E_{CT} directly relates to V_{oc} via Equation (1) (at 1 sun and room temperature), a very simple general, albeit mainly empirical, criterion for an efficient donor-acceptor blend is: $E_g - qV_{oc} > 0.6$ eV. Any attempt to bring V_{oc} closer to E_g will likely result in a loss of quantum efficiency for photoinduced electron transfer.[13,22] To the best of our

© 2012 WILEY-VCH Verlag GmbH & Co. KGaA, Weinheim

DOI: 10.1002/aenm.201200426

knowledge, no efficient organic solar cells have been described to date that violate this criterion, giving further credence to the validity of this design criterion. Of course it is important to find ways to lift this limitation, which is mainly governed by the large loss between E_{CT} and V_{oc}.[15] Suggestions for materials design that achieve high charge separation with less energetic losses have been proposed recently.[31,32] These include increasing the dielectric constant of the active layer materials or reducing the energetic disorder to enhance the charge carrier mobilities.

4. Experimental Section

Materials: PCBM, bis-PCBM, and ICBA were obtained from Solenne BV. The synthesis of PF10TBT,[33] t_2-bis-PCBM[18] and si-bis-PCBM[20] have been described previously.

Devices preparation and characterization: Photovoltaic devices were made by spin-coating PEDOT:PSS (Clevios P Al 4083) onto pre-cleaned, patterned indium tin oxide (ITO) substrates. The photoactive layer was deposited by spin coating from chlorobenzene solutions. The top electrode consisting of LiF (1 nm) and Al (80 nm) was deposited by vacuum evaporation at 1×10^{-6} mbar. Device characterization was performed under N_2 atmosphere. Current density-voltage measurements were carried out under illumination of a Steuernagel SolarConstant 1200 metal halide lamp, which was set to 1 sun intensity using a silicon reference cell and correcting for spectral mismatch. A computer-controlled Keithley 2400 was used as source meter.

Microscopy: Transmission electron microscopy was performed on a Tecnai G^2 Sphera TEM (FEI) operated at 200 kV. Bright field TEM images were acquired under slight defocusing conditions (see also Ref.16)

Photoluminescence and electroluminescence: Steady state photoluminescence and electroluminescence spectra were recorded at room temperature using an Edinburgh Instruments FLSP920 double-monochromator luminescence spectrometer equipped with a nitrogen-cooled near-IR sensitive photomultiplier (Hamamatsu). All spectra were corrected for the spectral response of the monochromators and photomultiplier. Fullerene solutions were prepared in toluene at 50 µg/mL and measured in 10 mm near-IR grade quartz cells at room temperature, with an optical density ~0.1 at the excitation wavelength. Thin films for PL were prepared by spin coating on quartz substrates using the same condition as for solar cell preparation. Electroluminescence was measured driving the solar cell in forward bias in a sealed box with a quartz window.

Time-resolved photoluminescence: Time-resolved photoluminescence measurements were performed on an Edinburgh Instruments LifeSpec-PS spectrometer using a 405 nm (3.06 eV) pulsed laser (PicoQuant PDL 800B) operated at 2.5 MHz with a pulse duration of 59 ps. For detection a Peltier-cooled Hamamatsu microchannel plate photomultiplier (R3809U-50) was used. Each intensity decay curve was fitted by a multi-exponential fit by reconvolution of the instrument response function (IRF) using $I(t) = \int_{-\infty}^{t} IRF(t') \sum_{i=1}^{n} A_i e^{-\frac{t-t'}{\tau_i}} dt'$, where A_i is the amplitude of the i^{th} component with a lifetime τ_i. The lifetime weighted fractional amplitude α_i corresponding to the lifetime τ_i is given by $\alpha_i = \frac{A_i \tau_i}{\sum A_i \tau_i}$.

Photoinduced absorption: Near steady-state photoinduced absorption (PIA) spectra were recorded between 0.35 and 2.4 eV by excitation with a mechanically modulated (275 Hz) laser source and by measuring the change in transmission of a tungsten-halogen probe beam through the sample (ΔT) with a phase sensitive lock-in amplifier after dispersion with a monochromator and detection using Si, InGaAs, and cooled InSb detectors. The pump wavelength used was 514 nm (2.41 eV, Ar ion laser) with a pump power of 25 mW and a beam diameter of 2 mm. The PIA signal ($-\Delta T/T$) was corrected for the photoluminescence, which was recorded in a separate experiment. All the spectra were corrected for the optical density at the pump wavelength. Thin films were prepared by spin coating from chlorobenzene solution and samples were held in an inert nitrogen atmosphere using an Oxford Optistat continuous flow cryostat during PIA measurements. Experiments were recorded at 290 and 80 K.

Acknowledgements

The work forms part of the research program of the Dutch Polymer Institute (DPI, projects #524, #631, # 660, and #678).

Received: June 9, 2012
Published online:

[1] For a review see: P. T. Boudreault, A. Najari, M. Leclerc, *Chem. Mater.* **2011**, *23*, 456.
[2] M. A. Green, K. Emery, Y. Hishikawa, W. Warta, E. D. Dunlop, *Prog. Photovolt: Res. Appl.* **2012**, *20*, 12.
[3] Y. Liang, Z. Xu, J. Xia, S.-T. Tsai, Y. Wu, G. Li, C. Ray, L. Yu, *Adv. Mater.* **2010**, *22*, E135.
[4] Z. He, C. Zhong, X. Huang, W.-Y. Wong, H. Wu, L. Chen, S. Su, Y. Cao, *Adv. Mater.* **2011**, *23*, 4636.
[5] L. Dou, J. You, J. Yang, C.-C. Chen, Y. He, S. Murase, T. Moriarty, K. Emery, G. Li, Y. Yang, *Nat. Photon.* **2012**, *6*, 180.
[6] V. D. Mihailetchi, P. W. M. Blom, J. C. Hummelen, M. T. Rispens, *J. Appl. Phys.* **2003**, *94*, 6849.
[7] L. J. A. Koster, V. D. Mihailetchi, R. Ramaker, P. W. M. Blom, *Appl. Phys. Lett.* **2005**, *86*, 123509.
[8] K. Vandewal, A. Gadisa, W. D. Oosterbaan, S. Bertho, F. Banishoeib, I. Van Severen, L. Lutsen, T. J. Cleij, D. Vanderzande, J. V. Manca, *Adv. Funct. Mater.* **2008**, *18*, 2064.
[9] M. Lenes, G. A. H. Wetzelaer, F. B. Kooistra, S. C. Veenstra, J. C. Hummelen, P. W. M. Blom, *Adv. Mater.* **2008**, *20*, 2116
[10] D. W. Laird, R. Stegamat, H. Richter, V. Vejins, L. Scott, T. A. Lada, Patent WO 2008/018931.
[11] Y. He, H. Chen, J. Hou, Y. Li, *J. Am. Chem. Soc.* **2010**, *132*, 1377.
[12] G. Zhao, Y. He, Y. Li, *Adv. Mater.* **2010**, *22*, 4355.
[13] D. Veldman, S. C. J. Meskers, R. A. J. Janssen, *Adv. Funct. Mater.* **2009**, *19*, 1939.
[14] M. A. Loi, S. Toffanin, M. Muccini, M. Forster, U. Scherf, M. Scharber, *Adv. Funct. Mater.* **2007**, *17*, 2111.
[15] K. Vandewal, K. Tvingstedt, A. Gadisa, O. Inganäs, J. V. Manca, *Nat. Mater.* **2009**, *8*, 904.
[16] M. Morana, H. Azimi, G. Dennler, H.-J. Egelhaaf, M. Scharber, K. Forberich, J. Hauch, R.Gaudiana, D. Waller, Z. Zhu, K. Hingerl, S. S. van Bavel, J. Loos, C. J. Brabec, *Adv. Funct. Mater.* **2010**, *20*, 1180.
[17] L. H. Slooff, S. C. Veenstra, J. M. Kroon, D. J. D. Moet, J. Sweelssen, M. M. Koetse, *Appl. Phys. Lett.* **2007**, *90*, 143506.
[18] R. K. M. Bouwer, J. C. Hummelen, *Chem. Eur. J.* **2010**, *16*, 11250.
[19] R. K. M. Bouwer, G. A. H. Wetzelaer, P. W. M. Blom, J. C. Hummelen, *J. Mater. Chem.* **2012**, *22*, 15412.
[20] R. K. M. Bouwer, *Fullerene bisadducts for organic photovoltaics*, PhD Thesis, Groningen University, **2012**.
[21] D. Veldman, Ö. pek, S. C. J. Meskers, J. Sweelssen, M. M. Koetse, S. C. Veenstra, J. M. Kroon, S. S. van Bavel, J. Loos, R. A. J. Janssen, *J. Am. Chem. Soc.* **2008**, *130*, 7721.
[22] M. A. Faist, T. Kirchartz, W. Gong, R. S. Ashraf, I. McCulloch, J. C. de Mello, N. J. Ekins-Daukes, D. D.C. Bradley, J. Nelson, *J. Am. Chem. Soc.* **2012**, *134*, 685.
[23] P. Wang, A. Abrusci, H. M. P. Wong, M. Svensson, M. R. Andersson, N. C. Greenham, *Nano Lett.* **2006**, *6*, 1789.

© 2012 WILEY-VCH Verlag GmbH & Co. KGaA, Weinheim

[24] H. M. P. Wong, P. Wang, A. Abrusci, M. Svensson, M. R. Andersson, N. C. Greenham, *J. Phys. Chem. C* **2007**, *111*, 5244.
[25] T. A. Ford, I. Avilov, D. Beljonne, N. C. Greenham, *Phys. Rev. B* **2005**, *71*, 125212.
[26] T. Offermans, P. A. van Hal, S. C. J. Meskers, M. M. Koetse, R. A. J. Janssen, *Phys. Rev. B* **2005**, *72*, 045213.
[27] S. Westenhoff, I. A. Howard, J. M. Hodgkiss, K. R. Kirov, H. A. Bronstein, C. K. Williams, N. C. Greenham, R. H. Friend, *J. Am. Chem. Soc.* **2008**, *130*, 13653.
[28] M. Liedtke, A. Sperlich, H. Kraus, A. Baumann, C. Deibel, M. J. M. Wirix, J. Loos, C. M. Cardona, V. Dyakonov, *J. Am. Chem. Soc.* **2011**, *133*, 9088.
[29] D. Di Nuzzo, A. Aguirre, M. Shahid, V. S. Gevaerts, S. C. J. Meskers, R. A. J. Janssen, *Adv. Mater.* **2010**, *22*, 4321.
[30] K. Vandewal, Z. Ma, J. Bergqvist, Z. Tang, E. Wang, P. Henriksson, K. Tvingstedt, M. R. Andersson, F. Zhang, O. Inganäs, *Adv. Funct. Mater.* **2012** DOI: 10.1002/adfm.201200608
[31] L. J. A. Koster, S. E. Shaheen, J. C. Hummelen, *Adv. Energy Mater.* **2012**, DOI: 10.1002/aenm.201200103.
[32] H. van Eersel, R. A. J. Janssen, M. Kemerink, *Adv. Funct. Mater.* **2012**, *22*, 2700.
[33] D. J. D. Moet, L. H. Slooff, J. M. Kroon, S. S. Chevtchenko, J. Loos, M. M. Koetse, J. Sweelssen, S. C Veenstra, *Mater. Res. Soc. Symp. Proc.* **2007**, *974*, 0974–CC03-09.

© 2012 WILEY-VCH Verlag GmbH & Co. KGaA, Weinheim